# Symbol Timing Estimation with CPM Modulation

Aldo N. D'Andrea, *Senior Member, IEEE*, Umberto Mengali, *Fellow, IEEE*, and Michele Morelli

***Abstract*— Symbol timing in continuous phase modulated signals is investigated making use of maximum likelihood estimation methods. Nondata-aided algorithms are proposed with a feedforward structure. They are suitable for digital implementation and can be employed with either full or partial response signaling. Multilevel symbol alphabets are allowed and the modulation index may be arbitrary. Performance is assessed by analysis and simulation. It turns out that full response schemes are comparatively easier to synchronize. Difficulties arise with partial response signaling, especially with long frequency pulses.**

## I. Introduction

CONTINUOUS phase modulation (CPM) is a signaling method that conserves and reduces energy and bandwidth at the same time. Furthermore, it generates constant envelope waveforms and therefore is very attractive in radio channels employing nonlinear power amplifiers. Notwithstanding these favorable features, current CPM applications are limited to few simple schemes (basically, MSK and its generalizations) because of implementation complexity and synchronization problems [1].

Implementation complexity has two different aspects. One arises from the large number of states needed to describe a CPM signal. In consequence, a maximum likelihood (ML) detector consists of a Viterbi algorithm operating on a generally large trellis. Methods to reduce the trellis size are discussed in [1]. The other aspect is related to the filter bank for the computation of the decoder metrics. The number of filters is established by the dimensionality of the signal space which may be large, especially with partial response and/or multilevel schemes. Again, methods to reduce this number without sacrificing error performance are referenced [1].

The other crucial issue with CPM signals is synchronization. In early studies [2], the IF signal is passed through a nonlinearity so as to generate tones, at carrier and clock frequencies, that are extracted by phase-locked loops (PLL's). With smoothed frequency pulses, however, this method fails because the amplitude of the tones is too small compared to the noise level. Even with large tones, anyway, the chance of false locks is a serious drawback.

References [3]–[7] discuss joint ML estimation of data sequence and carrier phase. Phase tracking algorithms are proposed that employ tentative decisions taken from a Viterbi decoder. Their application to general multilevel CPM signals results in good tracking performance. Acquisition times are rather long, however, and fast recovery schemes are still to be discovered.

Carrier frequency estimation is a subject of current intensive investigation and a few solutions are available either for MSK [8] and more general multilevel signaling [9].

Nondata-aided (NDA) timing recovery is discussed in [8] and [10]–[11] in the context of MSK-type modulations, i.e., binary alphabet with modulation index $h = 1/2$. A feedback scheme is proposed in [10], while references [8] and [11] are concerned with feedforward structures, which are more appealing for burst mode transmission. A decision-directed (DD) algorithm for general CPM modulation is investigated in [6]. It provides joint ML estimates of data, carrier phase and timing epoch. Unfortunately, the likelihood function to maximize has several local peaks. As the algorithm tends to settle on the peak most immediately uphill from the initial conditions, spurious locks may occur. Methods to overcome this problem involve a considerable increase in system complexity.

In this paper we consider timing synchronization for CPM digital modems. The received waveform is first filtered and then sampled at a fixed rate by a free-running oscillator. All further processing is done digitally. In particular the decision metrics for the decoder are computed by interpolating among samples [12]. This requires knowledge of the current timing epoch. We estimate this epoch following NDA methods. In this way any interaction between phase and timing recovery is eliminated. The resulting estimation scheme has a feedforward structure like that proposed in [13] for PAM modulation. Performance with full response signaling is good. Partial response formats, especially with long frequency pulses, are more difficult to cope with. It is likely that, in these cases, the only viable route is to resort to DD methods of the type described in [6].

The paper has the following outline. Signal model and basic notations are introduced in the next Section. Section III describes the timing estimation algorithm. Analytical methods to assess its performance are overviewed in Section IV. In this same Section, analytical and simulation results are compared. Some conclusions are offered in Section V.

## II. Signal Model

The complex envelope of the received waveform is composed of signal plus noise

$$r(t) = s(t) + w_R(t) + jw_I(t). \tag{1}$$

The noise is Gaussian and has independent real and imaginary components, $w_R(t)$ and $w_I(t)$, each with power spectral

Paper approved by E. Panayirci, the Editor for Synchronization and Equalization of the IEEE Communications Society. Manuscript received April 27, 1995; revised January 23, 1996.

The authors are with the Department of Information Engineering, University of Pisa, Italy.

Publisher Item Identifier S 0090-6778(96)07081-X.

density $N_0$. The signal has the form

$$s(t) = \sqrt{\frac{2E_s}{T}} e^{j[\theta + \psi(\boldsymbol{\alpha}; t-\tau)]} \tag{2}$$

where $E_s$ represents the energy per signaling interval, $T$ is the symbol period, $\theta$ and $\tau$ are carrier phase and timing epoch, respectively, $\boldsymbol{\alpha} = \{\alpha_i\}$ is the data sequence and $\psi(\boldsymbol{\alpha}; t)$ is the information bearing phase

$$\psi(\boldsymbol{\alpha}; t) = 2\pi h \sum_i \alpha_i q(t - iT). \tag{3}$$

The parameter $h$ is the modulation index and $q(t)$ is the *phase pulse* of the modulator, which is related to the *frequency pulse* $g(t)$ by

$$q(t) = \int_{-\infty}^{t} g(\tau)\, d\tau. \tag{4}$$

In this study, we assume that data symbols are equally likely, independent, and belong to an $M$-ary alphabet $\{\pm 1, \pm 3, \cdots, \pm(M-1)\}$. Pulse $g(t)$ is time limited to the interval $(0, LT)$ and is normalized so that $q(LT) = 1/2$. In numerical examples discussed later, two specific forms of $g(t)$ are used: rectangular of length $L$ (LREC) and raised-cosine of length $L$ (LRC). With these pulses it is easily seen that $q(t)$ satisfies the symmetry condition

$$q(t) = \tfrac{1}{2} - q(LT - t). \tag{5}$$

In a digital implementation of the receiver the incoming waveform is first passed through an anti-aliasing filter (AAF) and then is sampled at some rate $1/T_s$. The filter bandwidth $B_{\text{AAF}}$ must be large enough not to distort the signal components and the sampling rate must exceed $2B_{\text{AAF}}$ to avoid aliasing. In the following we also assume that: 1) the AAF transfer function is rectangular, 2) $1/T_s$ is a multiple $N$ of the symbol rate, and 3) the AAF bandwidth equals $1/2T_s$; in other words, $B_{\text{AAF}} = N/2T$. These restrictions will be relaxed later, when the timing algorithm has been identified.

To proceed, let $x(t)$ be the output of AAF and denote $x(k)$ its samples taken at $t = kT_s, k = 0, 1, 2 \cdots$ As the signal is not distorted in passing through AAF, we have

$$x(k) = \sqrt{\frac{2E_s}{T}} e^{j[\theta + \psi(\boldsymbol{\alpha}; kT_s - \tau)]} + n_R(k) + j n_I(k). \tag{6}$$

Due to the previous hypotheses, $\{n_R(k)\}$ and $\{n_1(k)\}$ are independent and white random sequences. Also, $n_R(k)$ and $n_I(k)$ have the same variance $\sigma_n^2 = N_0/T_s$.

As the signal component in (6) depends on $\boldsymbol{\alpha}, \theta$ and $\tau$, we may estimate all these parameters from the observation of $\{x(k)\}$. In this study, however, we are only concerned with timing estimation and, accordingly, we consider data and carrier phase as *nuisance* parameters. In other words, we look for NDA and phase-independent timing algorithms. Our search is based on maximum likelihood methods. In particular, the sequence is divided into adjoining segments $\{x(k)\}^{(l)}$ $(l = 0, 1, 2, \cdots)$ of $N \times L_0$ elements, and each segment is independently processed to get an estimate $\hat{\tau}^{(l)}$ of $\tau$. All these estimates are then employed to control the interpolation/detection operations with methods similar to those described in [12]–[13] for PAM modulation.

## III. Timing Algorithm

### A. Derivation of the Likelihood Function

For simplicity, we concentrate on the first segment of $\{x(k)\}$ and omit the index $l$ throughout. Letting $\boldsymbol{x} = \{x(0), x(1), \cdots x(NL_0 - 1)\}$ be the samples in the segment, consider the likelihood function for the unknown parameters $\boldsymbol{\alpha}, \theta$ and $\tau$. This function is readily derived from (6), bearing in mind that the noise samples are independent

$$\Lambda(\boldsymbol{x}|\tilde{\boldsymbol{\alpha}}, \tilde{\theta}, \tilde{\tau}) = \exp\left\{ -\frac{1}{2\sigma_n^2} \sum_{k=0}^{NL_0-1} \left| x(k) - \sqrt{\frac{2E_s}{T}} e^{j[\tilde{\theta} + \psi(\tilde{\boldsymbol{\alpha}}; kT_s - \tilde{\tau})]} \right|^2 \right\}. \tag{7}$$

The quantities $\tilde{\boldsymbol{\alpha}}, \tilde{\theta}$ and $\tilde{\tau}$ in (7) represent trial values of $\boldsymbol{\alpha}, \theta$ and $\tau$. Equation (7) may be simplified by pruning off constants independent of $\tilde{\boldsymbol{\alpha}}, \tilde{\theta}$ and $\tilde{\tau}$. Noting that

$$\left| x(k) - \sqrt{\frac{2E_s}{T}} e^{j[\tilde{\theta} + \psi(\tilde{\boldsymbol{\alpha}}; kT_s - \tilde{\tau})]} \right|^2 = |x(k)|^2 + \frac{2E_s}{T} - 2\sqrt{\frac{2E_s}{T}} \operatorname{Re}\{x(k) e^{-j[\tilde{\theta} + \psi(\tilde{\boldsymbol{\alpha}}; kT_s - \tilde{\tau})]}\} \tag{8}$$

this results in the equivalent likelihood function

$$\Lambda_1(\boldsymbol{x}|\tilde{\boldsymbol{\alpha}}, \tilde{\theta}, \tilde{\tau}) = \exp\left\{ \frac{1}{\sigma_n^2} \sqrt{\frac{2E_s}{T}} \operatorname{Re} \cdot \left[ e^{-j\tilde{\theta}} \sum_{k=0}^{NL_0-1} x(k) e^{-j\psi(\tilde{\boldsymbol{\alpha}}; kT_s - \tilde{\tau})} \right] \right\}. \tag{9}$$

As mentioned earlier, we are not interested in $\Lambda_1(\boldsymbol{x}|\tilde{\boldsymbol{\alpha}}, \tilde{\theta}, \tilde{\tau})$ in itself. Data symbols and carrier phase are nuisance parameters. So, what we really need is the *marginal* likelihood function of $\tau$, which is obtained by averaging out $\tilde{\theta}$ and $\tilde{\boldsymbol{\alpha}}$ from $\Lambda_1(\boldsymbol{x}|\tilde{\boldsymbol{\alpha}}, \tilde{\theta}, \tilde{\tau})$. To this end let us define

$$X(\tilde{\boldsymbol{\alpha}}, \tilde{\tau}) \triangleq \sum_{k=0}^{NL_0-1} x(k) e^{-j\psi(\tilde{\boldsymbol{\alpha}}; kT_s - \tilde{\tau})} \tag{10}$$

and denote $\varphi$ the argument of $X(\tilde{\boldsymbol{\alpha}}, \tilde{\tau})$. Then, (9) becomes

$$\Lambda_1(\boldsymbol{x}|\tilde{\boldsymbol{\alpha}}, \tilde{\theta}, \tilde{\tau}) = \exp\left\{ \sqrt{\frac{2E_s}{T}} \frac{|X(\tilde{\boldsymbol{\alpha}}, \tilde{\tau})|}{\sigma_n^2} \cos(\varphi - \tilde{\theta}) \right\}. \tag{11}$$

Hence, assuming $\tilde{\theta}$ uniformly distributed over $(-\pi, \pi)$ and averaging $\Lambda_1(\boldsymbol{x}|\tilde{\boldsymbol{\alpha}}, \tilde{\theta}, \tilde{\tau})$ with respect to $\tilde{\theta}$ yields

$$\Lambda_2(\boldsymbol{x}|\tilde{\boldsymbol{\alpha}}, \tilde{\tau}) = I_0\left( \sqrt{\frac{2E_s}{T}} \frac{|X(\tilde{\boldsymbol{\alpha}}, \tilde{\tau})|}{\sigma_n^2} \right) \tag{12}$$

where $I_0(\lambda)$ is the modified Bessel function of zero order.

Elimination of $\tilde{\boldsymbol{\alpha}}$ from $\Lambda_2(\boldsymbol{x}|\tilde{\boldsymbol{\alpha}}, \tilde{\tau})$ is a much more difficult problem and all our attempts to solve it encountered impassable barriers. The only way we see to overcome the obstacle

is to assume a low SNR and, making the approximation $I_0(\lambda) \cong 1 + \lambda^2/4$, to transform (12) into

$$\Lambda_2(\boldsymbol{x}|\tilde{\boldsymbol{\alpha}}, \tilde{\tau}) \cong 1 + \frac{E_s}{2T} \frac{|X(\tilde{\boldsymbol{\alpha}}, \tilde{\tau})|^2}{\sigma_n^4}. \tag{13}$$

In these conditions, dropping the additive constant and the immaterial factor $E_s/2T\sigma_n^4$ yields

$$\Lambda_3(\boldsymbol{x}|\tilde{\boldsymbol{\alpha}}, \tilde{\tau}) \cong |X(\tilde{\boldsymbol{\alpha}}, \tilde{\tau})|^2. \tag{14}$$

It is worth noting that this same approach has already been followed in the literature [14]–[15] as it leads to closed form solutions that would probably be hindered by more accurate developments. It is fair to say, however, that in most applications the SNR is not so low as to justify (13) and the question of the exact ML timing estimator remains a challenging object of further study.

Substituting (10) into (14) and taking the average with respect to $\tilde{\boldsymbol{\alpha}}$ yields

$$\Lambda_4(\boldsymbol{x}|\tilde{\tau}) = \sum_{k_1=0}^{NL_0-1} \sum_{k_2=0}^{NL_0-1} x(k_1)x^*(k_2)F[(k_2-k_1)T_s, k_2T_s - \tilde{\tau}] \tag{15}$$

which is the desired *marginal* likelihood function. Here, $F(\Delta t, t)$ is the expectation of the exponential $e^{j[\psi(\tilde{\boldsymbol{\alpha}};t)-\psi(\tilde{\boldsymbol{\alpha}};t-\Delta t)]}$ over the data symbols. An explicit expression for $F(\Delta t, t)$ is found with the methods in [10] and reads

$$F(\Delta t, t) = \prod_{i=-\infty}^{\infty} \frac{1}{M} \frac{\sin[2h\pi M p_{\Delta t}(t-iT)]}{\sin[2h\pi p_{\Delta t}(t-iT)]} \tag{16}$$

where $M$ is the size of the symbol alphabet and $p_{\Delta t}(t)$ is related to the phase response of the modulator by

$$p_{\Delta t}(t) = q(t) - q(t-\Delta t). \tag{17}$$

It is worth noting that $F(\Delta t, t)$ is a periodic function of $t$ with period $T$ and, as such, it needs to be computed only on one symbol interval, say $t \in (0, T)$. Furthermore, it can be shown that almost all the factors in (16) are unity. Indeed, for $t \in (0, T)$ and $\Delta t > 0$, the only nonunity factors are those with the index in the range $-[L + \text{int}(\Delta t/T)] \leq i \leq 0$, where $\text{int}(\Delta t/T)$ means "largest integer not exceeding $\Delta t/T$."

Our ultimate goal will be the computation of the argument $\tilde{\tau}$ that maximizes $\Lambda_4(\boldsymbol{x}|\tilde{\tau})$. It is clear from (15), however, that this is a difficult task because the cumbersome form of $F(\Delta t, t)$ prevents a straightforward calculation and, what is more, function $\Lambda_4(\boldsymbol{x}|\tilde{\tau})$ might have several maxima. To proceed, we expand $F(\Delta t, t)$ into a Fourier series in the hope that only few terms in the series are significant. This leads us to write $F[\cdot, \cdot]$ in (15) in the form

$$F[(k_2-k_1)T_s, k_2T_s - \tilde{\tau}] = \sum_{m=-\infty}^{\infty} C_m(k_1, k_2) e^{j2\pi m\tilde{\tau}/T}. \tag{18}$$

In the Appendix A, it is shown that the coefficients $C_m(k_1, k_2)$ are given by

$$C_m(k_1, k_2) = h_m(k_1 - k_2) e^{-j\pi m(k_1+k_2)/N} \tag{19}$$

where $h_m(k)$ is an even and real valued function

$$h_m(k) \triangleq e^{j\pi mk/N} \frac{1}{T} \int_0^T F(-kT_s, u) e^{j2\pi mu/T}\, du \tag{20}$$

that satisfies the relationship

$$h_{-m}(k) = h_m(k). \tag{21}$$

Substituting these results into (15) and performing some algebraic manipulations (see again Appendix A), yields

$$\Lambda_5(\boldsymbol{x}|\tilde{\tau}) = \text{Re}\left\{ \sum_{m=1}^{\infty} A(m) e^{j2\pi m\tilde{\tau}/T} \right\} \tag{22}$$

with

$$A(m) \triangleq \sum_{k=0}^{NL_0-1} [x(k)e^{-j\pi mk/N}] y_m^*(k) \tag{23}$$

$$y_m(k) \triangleq \sum_{i=0}^{NL_0-1} [x(i)e^{j\pi mi/N}] h_m(k-i). \tag{24}$$

At this point the question arises of how many terms in the sum (22) are significant. To address this problem, we look at $h_m(k)$ as a sampled version of the continuous-time function

$$h_m(t) = e^{j\pi mt/T} \frac{1}{T} \int_0^T F(-t, u) e^{j2\pi mu/T}\, du \tag{25}$$

with $t = kT_s, k = 0, 1, 2, \cdots$. Fig. 1 illustrates the shape of $h_m(t)$ for 1REC pulses, binary symbols ($M = 2$) and $h = 1/2$. As is seen, functions $h_m(t) (m = 1, 2, 3)$ are all even and $h_1(t)$ is, by far, the largest. This would suggest keeping only the first term in (22), but it is not clear whether such an approximation has a general validity. An answer comes from Tables I and II which show the ratio of the energy of $h_m(t)$, say $E_m$, to the energy of $h_1(t)$ for a few LREC and LRC formats. It appears that with binary symbols $h_1(t)$ is dominating even for $h \neq 1/2$. With quaternary and octal alphabets, instead, this is not true unless $h$ is small. Based on these observations we conjecture that (22) can be approximated with the first term when either $M = 2$ or $M > 2$ and $h$ is small.

### B. Practical Adjustments

In many practical cases the observation interval is much longer than the symbol interval ($L_0 \gg 1$) and (23) may be rearranged in a more convenient form. Looking at Fig. 1 it is seen that $h_m(t)$ is very short (two symbol intervals to right and left of the origin). As $h_m(t)$ is short even with other modulation formats, we expect that (24) is only marginally affected by extending the summation from $-\infty$ to $+\infty$. This transforms the right hand side into a convolution $[x(k)e^{j\pi mk/N}] \otimes h_m(k)$ and the signal $y_m(k)$ may be viewed as the output of a (noncausal) real filter driven by $x(k)e^{j\pi mk/N}$. The filter can be made causal by shifting $h_m(k)$

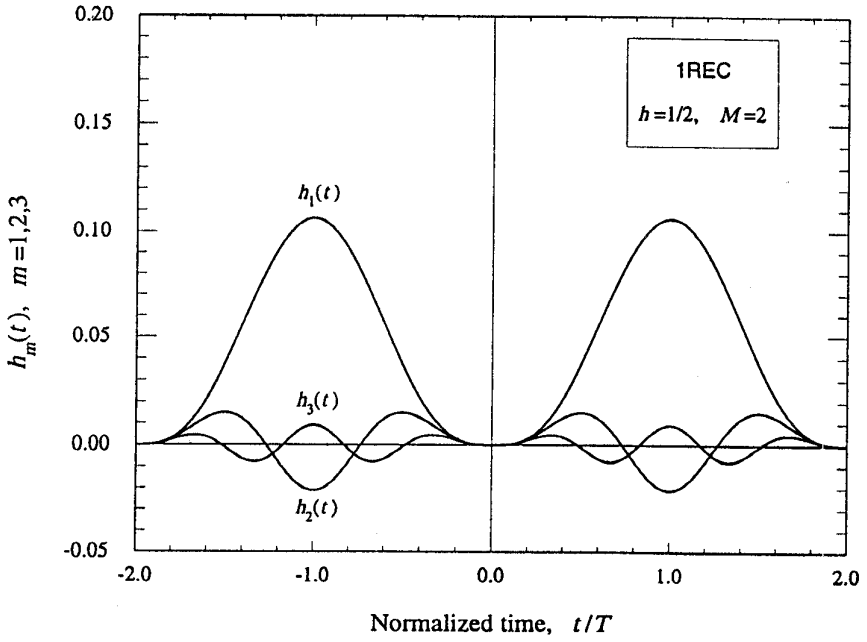


Fig. 1. Shape of $h_m(t)$ for 1REC pulses, binary symbols and $h = 1/2$.

TABLE I
RATIO $E_m/E_1$ FOR SOME LREC FORMATS

| $M$ | $h$ | $L$ | $E_2/E_1$ | $E_3/E_1$ | $E_4/E_1$ |
|---|---|---|---|---|---|
| 2 | 1/2 | 1 | 3.40E-02 | 6.05E-03 | 1.85E-03 |
| 2 | 1/2 | 2 | 4.33E-02 | 8.09E-03 | 2.51E-03 |
| 2 | 4/5 | 1 | 8.10E-03 | 1.22E-03 | 3.52E-04 |
| 2 | 4/5 | 2 | 9.46E-03 | 1.56E-03 | 4.67E-04 |
| 4 | 1/4 | 1 | 3.00E-02 | 5.32E-03 | 1.61E-03 |
| 4 | 1/2 | 1 | 2.57E-01 | 1.91E-02 | 4.70E-03 |
| 4 | 4/5 | 1 | 4.50E-01 | 4.25E-01 | 4.12E-02 |
| 8 | 1/8 | 1 | 3.06E-02 | 5.31E-03 | 1.61E-03 |
| 8 | 1/4 | 1 | 2.62E-01 | 2.00E-02 | 4.89E-03 |
| 8 | 2/5 | 1 | 5.03E-01 | 3.00E-01 | 3.35E-02 |
| 8 | 1/2 | 1 | 4.98E-01 | 3.31E-01 | 1.72E-01 |

TABLE II
RATIO $E_m/E_1$ FOR SOME LRC FORMATS

| $M$ | $h$ | $L$ | $E_2/E_1$ | $E_3/E_1$ | $E_4/E_1$ |
|---|---|---|---|---|---|
| 2 | 1/2 | 1 | 1.80E-02 | 1.08E-04 | 4.33E-06 |
| 2 | 1/2 | 2 | 3.55E-04 | 2.76E-06 | 2.01E-07 |
| 2 | 4/5 | 1 | 3.55E-02 | 7.17E-04 | 1.13E-05 |
| 2 | 4/5 | 2 | 4.46E-04 | 4.67E-07 | 1.43E-08 |
| 4 | 1/4 | 1 | 1.85E-02 | 2.27E-04 | 5.79E-06 |
| 4 | 1/2 | 1 | 1.36E-01 | 1.20E-02 | 6.09E-04 |
| 4 | 4/5 | 1 | 3.80E-01 | 1.11E-01 | 1.83E-02 |
| 8 | 1/8 | 1 | 1.88E-02 | 2.76E-04 | 6.25E-06 |
| 8 | 1/4 | 1 | 1.29E-01 | 1.09E-02 | 6.54E-04 |
| 8 | 2/5 | 1 | 2.86E-01 | 7.78E-02 | 1.34E-02 |
| 8 | 1/2 | 1 | 2.88E-01 | 1.22E-01 | 3.76E-02 |

rightward. In the sequel we shift $h_m(k)$ by $ND$ steps and choose $D$ as the smallest integer such that $h_m(k)$ is confined within the interval $-ND \leq k \leq ND$, whatever is $m$. For example, $D = 2$ is an appropriate choice in the case of Fig. 1.

Shifting $h_m(k)$ rightward implies delaying the filter output by the same amount. Hence

$$y_m(k - ND) = [x(k)e^{j\pi mk/N}] \otimes h_m(k - ND) \tag{26}$$

and (23) may be rearranged as

$$A(m) = \sum_{k=ND}^{N(L_0+D)-1} \cdot [x(k - ND)e^{-j\pi m(k-ND)/N}]y_m^*(k - ND). \tag{27}$$

Fig. 2 gives a pictorial interpretation of this equation.

### C. Timing Epoch Estimation

Next, we look for the value of $\tilde{\tau}$ that maximizes $\Lambda_5(\boldsymbol{x}|\tilde{\tau})$. In general, no closed form solution is available, except when the sum (22) can be truncated to the first term

$$\Lambda_5(\boldsymbol{x}|\tilde{\tau}) \cong \mathrm{Re}\{A(1)e^{j2\pi\tilde{\tau}/T}\}. \tag{28}$$

In these circumstances, the maximum is clearly achieved for

$$\hat{\tau} = -\frac{T}{2\pi}\arg\{A(1)\}. \tag{29}$$

Equation (29) is strongly reminiscent of other estimation methods proposed in the literature. In fact, it corresponds to the scheme in [6] when the data symbols are averaged out so as to pass from a decision-directed to a nondata-aided algorithm. Also, it formally coincides with the estimation equation obtained in [15] for PAM signaling, where $A(1)$

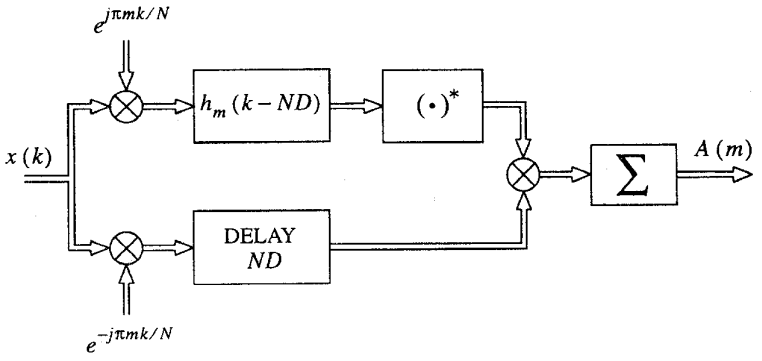


Fig. 2. Illustrating the computation of $A(m)$.

represents the Fourier transform of the squared samples from the matched filter as computed at $f = 1/T$.

The more general case can be approached by a recursive search. Suppose that the sum (22) can be approximated by the first $Q$ terms and let $\Lambda_5'(\boldsymbol{x}|\tilde{\tau})$ and $\Lambda_5''(\boldsymbol{x}|\tilde{\tau})$ be first and second derivatives of $\Lambda_5(\boldsymbol{x}|\tilde{\tau})$ with respect to $\tilde{\tau}$. It is easily shown that

$$\Lambda_5'(\boldsymbol{x}|\tilde{\tau}) = -\frac{2\pi}{T}\mathrm{Im}\left\{\sum_{m=1}^{Q} mA(m)e^{j2\pi m\tilde{\tau}/T}\right\} \tag{30}$$

$$\Lambda_5''(\boldsymbol{x}|\tilde{\tau}) = -\left(\frac{2\pi}{T}\right)^2 \mathrm{Re}\left\{\sum_{m=1}^{Q} m^2A(m)e^{j2\pi m\tilde{\tau}/T}\right\}. \tag{31}$$

Then, the following recursion may be employed

$$\hat{\tau}_{n+1} = \hat{\tau}_n - \frac{\Lambda_5'(\boldsymbol{x}|\hat{\tau}_n)}{E_x\{\Lambda_5''(\boldsymbol{x}|\tilde{\tau}=\tau)\}}, \qquad n = 0, 1, 2, \cdots \tag{32}$$

where the initial $\hat{\tau}_0$ value is taken from (29) and $E_x\{\Lambda_5''(\boldsymbol{x}|\tilde{\tau} = \tau)\}$ denotes statistical expectation of $\Lambda_5''(\boldsymbol{x}|\tilde{\tau})$ given $\tilde{\tau} = \tau$. The reason for using the expectation of $\Lambda_5''(\boldsymbol{x}|\tilde{\tau})$ instead of $\Lambda_5''(\boldsymbol{x}|\tilde{\tau})$ itself is to ease the computation load. In this way, in fact, the denominator becomes a constant whose expression is found to be

$$E_x\{\Lambda_5''(\boldsymbol{x}|\tilde{\tau}=\tau)\} = -\left(\frac{2\pi}{T}\right)^2 \frac{2E_s}{T} NL_0 \sum_{m=1}^{Q} m^2 \left[\sum_{k=-\infty}^{\infty} h_m^2(k)\right]. \tag{33}$$

### D. Remarks

So far, several questions have been left aside to avoid unnecessary detours. At this stage, however, the timing algorithm has been identified and we may retrace our steps to comment on some important issues. We start from (32) and proceed backward.

1) One interesting point about this equation is whether $\hat{\tau}_n$ converges to the abscissa of the *absolute maximum* of $\Lambda_5(\boldsymbol{x}|\tilde{\tau})$. As observed earlier, $\Lambda_5(\boldsymbol{x}|\tilde{\tau})$ might have several peaks and it is not obvious from the form of (32) that the highest peack will eventually be reached. Extensive simulations have shown that the highest peack is always attained.
2) The number of iterations needed in (32) is of some concern. We have found by simulation that one or two iterations are sufficient to practically achieve the limit $\hat{\tau}_\infty$.
3) It follows from 2) that the greater complexity of (32) with respect to (29) is in the computation of $A(m), m = 2, \cdots Q$. Again, simulations tell us that $Q$ can be limited to three, in the worst cases. No performance improvements have been observed letting $Q > 3$.
4) Estimates resulting from (29) or (32) are based on one segment of $\{x(k)\}$. In general, let us denote $\hat{\tau}^{(l)}$ the estimate pertaining to $\{x(k)\}^{(l)}$. As $\Lambda_5(\boldsymbol{x}|\tilde{\tau})$ is a periodic function of period $T$, the abscissa where the maximum is located can only be computed within multiples of one symbol period. Thus, additional post-processing on $\hat{\tau}^{(l)}, l = 0, 1, 2\cdots$, is needed to eliminate discontinuities from one estimate to the next. This is a manifestation of the so-called *unwrapping problem* which has been thoroughly discussed in [13]. There, final estimates of the type

$$\hat{\tau}_{\text{final}}^{(l+1)} = \hat{\tau}_{\text{final}}^{(l)} + \text{saw}(\hat{\tau}^{(l)} - \hat{\tau}_{\text{final}}^{(l)}), \quad l = 0, 1, 2\cdots \tag{34}$$

have been proposed, where $\text{saw}(\hat{\tau})$ is a sawtooth nonlinearity that reduces $\hat{\tau}$ to the interval $\pm T/2$. In the simulations reported later, this post-processing has been adopted.
5) Timing estimates $\hat{\tau}^{(l)}$ $(l = 0, 1, 2, \cdots)$ are generally dependent on each other. To see why, let us observe that $A^{(l)}(m)$ is a function of $\{[x(k)e^{j\pi mk/N}] \otimes h_m(k - ND)\}^{(l)}$ (see (26)–(27)). Now, as $h_m(k - ND)$ has a duration of $2ND$, it follows that $A^{(l)}(m)$ depends not only on $\{x(k)\}^{(l)}$ but also on the last $2ND$ elements of $\{x(k)\}^{(l-1)}$. Thus, $A^{(l-1)}(m)$ and $A^{(l)}(m)$ are correlated. In many practical cases $L_0$ is much greater than $2D$ and the correlation is weak, however.
6) Another way to state the above is to say that we need more than just $NL_0$ samples to compute $\hat{\tau}^{(l)}$. Actually we need $NL_0'$ such samples, with

$$L_0' = L_0 + 2D. \tag{35}$$

This is an important point when comparing estimates (29) and (32) with the modified Cramer-Rao bound [16]. In fact this bound is a function of the length of the observation interval in symbol intervals, $L_0'$, and reads

either

$$\mathrm{MCRB} = \frac{3L}{2L_0'\pi^2 h^2(M^2-1)}\left(\frac{E_s}{N_0}\right)^{-1} \tag{36}$$

or

$$\mathrm{MCRB} = \frac{L}{L_0'\pi^2 h^2(M^2-1)}\left(\frac{E_s}{N_0}\right)^{-1} \tag{37}$$

depending on whether LREC or LRC pulses are considered.

7) Intuitively, the performance of the estimators (29) and (32) improves as $L_0$ increases. So, one wonders whether $L_0$ may be made arbitrarily large. One limit to $L_0$ comes from the assumption that the symbol period is a multiple of the sampling period, $T_s = T/N$. To see why, bear in mind that sampling commands come from a free running oscillator, whose frequency cannot be exactly a multiple of the clock rate. So, suppose that $1/T_s$ is offset by $\Delta f$ from its ideal value. Then, the oscillator will gain or lose $\Delta f$ cycles per second or (which is the same) will be in error by a fraction $\Delta f L_0 T_s$ of symbol period every $L_0$ symbols. What happens if the fraction is small? Things go as if the relationship $T_s = T/N$ were exactly true but the timing epoch $\tau$ were a (slowly) varying function of time. In conclusion, the assumption $T_s = T/N$ is approximately valid provided that $\Delta f L_0 T_s$ is much less than unity, say less than $10^{-2}$. For example, for $\Delta f = 5 \times 10^{-5}/T_s$, this happens with $L_0 \leq 200$.
8) The choice of the oversampling factor $N$ is another crucial issue as it affects the accuracy of the estimates. Simulations indicate that (29) and (32) give unbiased estimates only if $N$ is not less than some minimum $N_{\min}$ which depends on the signal bandwidth. Counting positive frequencies only, let $2B_{99.9\%}$ be the RF bandwidth containing 99.9% of the signal power. Then the following rule-of-thumb formula has been found

$$N_{\min} \geq \frac{3}{2} T \times B_{99.9\%}. \tag{38}$$

In particular, $N_{\min} = 4$ is adequate with binary modulation. With quaternary or octal modulations, instead, $N_{\min} = 4$ is sufficient only with small modulation indexes (say, $h \leq 1/2$ for $M = 4$ and $h \leq 1/4$ for $M = 8$). Otherwise, larger values of $N_{\min}$ are needed.
9) A rectangular shape for the AAF transfer function is not realizable. In the simulations illustrated later we have adopted an eight-pole Butterworth FIR filter. Its 3 dB bandwidth is taken as the AAF bandwidth $B_{\mathrm{AAF}}$. As a rule, $B_{\mathrm{AAF}}$ has been related to the oversampling factor as follows

$$B_{\mathrm{AAF}} = \frac{N}{2T}. \tag{39}$$

## IV. Performance

In this Section we discuss the performance of the estimators (29) and (32). Analysis is limited to (29) for no viable route has been found to deal with (32). Indeed, the performance of (32) has only been addressed by simulation. Performance of timing algorithms is expressed in terms of mean value $E\{\hat{\tau}/T\}$ and variance $\sigma^2$ of the estimates, as normalized to the symbol period. Estimates must be unbiased (meaning that $E\{\hat{\tau}\} = \tau$) and the standard deviation $\sigma$ must be much less than unity to keep degradations in symbol error probability within acceptable limits.

The computation of $E\{\hat{\tau}/T\}$ and $\sigma^2$ for the algorithm (29) proceeds as follows. As $\hat{\tau}$ is proportional to the argument of $A(1)$, we expect that $A(1)$ will undergo small fluctuations around its average $\overline{A}(1)$ under good operating conditions. Letting

$$\frac{A(1) - \overline{A}(1)}{\overline{A}(1)} = \delta_R + j\delta_I \tag{40}$$

this implies that $\delta_R$ and $\delta_I$ are much smaller than unity. Then, solving (40) for $A(1)$ and neglecting $\delta_R$ yields

$$A(1) \cong \overline{A}(1)(1 + j\delta_I) \tag{41}$$

from which, substituting into (29), yields

$$\hat{\tau} \cong -\frac{T}{2\pi}\arg\{\overline{A}(1)\} - \frac{T}{2\pi}\delta_I. \tag{42}$$

It is easily seen from (40) that $\delta_I$ has zero mean. Hence, the mean value of $\hat{\tau}$ equals the first term in (42) or, in other words

$$E\left\{\frac{\hat{\tau}}{T}\right\} = -\frac{1}{2\pi}\arg\{\overline{A}(1)\}. \tag{43}$$

Also, the timing error variance (normalized to the symbol period) is given by

$$\sigma^2 = \frac{1}{4\pi^2}E\{\delta_I^2\}. \tag{44}$$

Computation of $E\{\hat{\tau}/T\}$ and $\sigma^2$ in (43)–(44) is a straightforward but very cumbersome task. Basically, the method used in [13] may be followed. Due to lack of space we give only the final results here.

Let us begin with $E\{\hat{\tau}/T\}$. The average of $A(1)$ is found to be

$$\overline{A}(1) = \frac{2E_s}{T}NL_0 \sum_{k=-\infty}^{\infty}\sum_{l=-\infty}^{\infty}(-1)^{kl} \cdot h_1(k)h_{1+lN}(k)e^{-j2\pi(1+lN)\tau/T}. \tag{45}$$

Inspection of (45) indicates that $\overline{A}(1)$ is independent of the noise level and, accordingly, so is the average of $\hat{\tau}$. In general, the argument of $\overline{A}(1)$ is not proportional to $\tau$, as is desirable to get unbiased estimates. In the previous Section we have seen, however, that the energy of $h_m(k)$ decreases as the index $m$ increases in amplitude. Thus, if the oversampling factor $N$ is large enough so that the functions $h_{1+lN}(k)$ with $l \neq 0$ are all negligible with respect to $h_1(k)$, then (45) reduces to

$$\overline{A}(1) \approx e^{-j2\pi\tau/T} \times \frac{2E_s}{T}NL_0 \sum_{k=-\infty}^{\infty} h_1^2(k) \tag{46}$$

and its substitution in (43) yields $E\{\hat{\tau}\} = \tau$.

Intuitively, the conditions for (46) to hold depend on the modulation format. Simulations indicate that $N$ must exceed

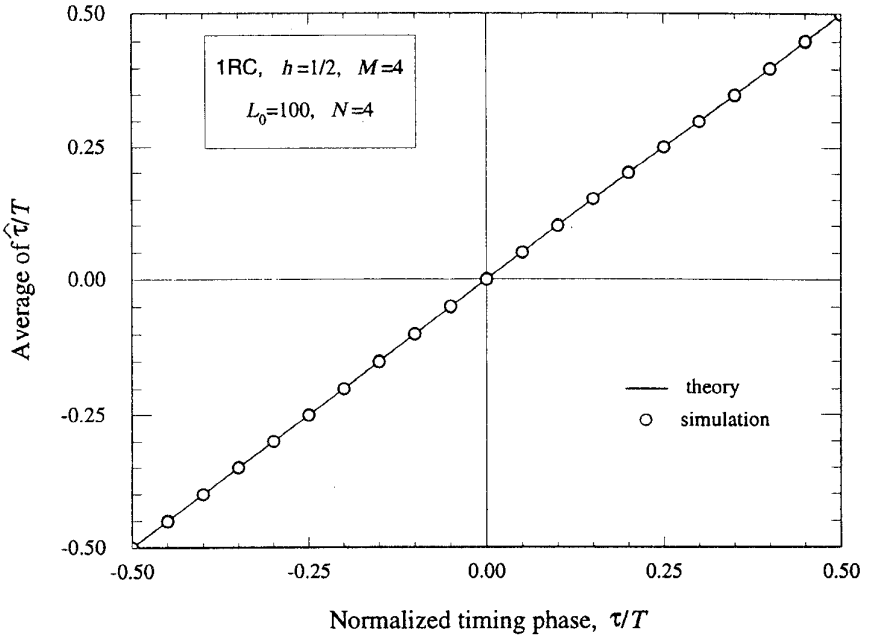


Fig. 3. Average value of $\hat{\tau}/T$ versus $\tau/T$ with quaternary modulation, 1RC pulses and $h = 1/2$.

some minimum which depends on the signal bandwidth according to the empirical formula (38). A factor $N = 4$ is sufficient with a binary alphabet, whatever the modulation index. It is also sufficient with multilevel signaling provided that the modulation index is limited. For example, Fig. 3 displays simulations for $E\{\hat{\tau}/T\}$ versus $\tau/T$ with $N = 4$, quaternary modulation and $h = 1/2$. The solid line represents the equation $E\{\hat{\tau}/T\} = \tau/T$. As is seen, deviations from the ideal result are so small than cannot be appreciated from the graph. In fact they are on the order of $3 \times 10^{-4}$.

The variance of the estimate $\hat{\tau}/T$ is found as the sum of three terms

$$\sigma^2 = \frac{K_{NN}}{L_0}\left(\frac{E_s}{N_0}\right)^{-2} + \frac{K_{SN}}{L_0}\left(\frac{E_s}{N_0}\right)^{-1} + \frac{K_{SS}}{L_0} \qquad (47)$$

corresponding to interactions noise $\times$ noise, signal $\times$ noise, and signal $\times$ signal. The self-noise term $K_{SS}/L_0$ represents the asymptotic value of $\sigma^2$ when $E_s/N_0$ increases. The coefficients $K_{NN}, K_{SN}$ and $K_{SS}$ have rather awkward expressions given in Appendix B. In general, they are functions of: 1) modulation format, 2) AAF bandwidth, 3) timing epoch, and 4) observation interval $L_0$. Actually, the dependence of $K_{NN}$ and $K_{SN}$ on $\tau$ and $L_0$ is so weak that it can be ignored for practical purposes. This is not true with $K_{SS}$ which, in many cases, is inversely proportional to $L_0$. No simple rule has been identified relating $K_{SS}$ to $\tau$. However, as the influence of $\tau$ on the overall variance $\sigma^2$ is visible only at large signal-to-noise ratios (say, $E_s/N_0 > 20$ dB), the numerical results reported in the sequel are given only for $\tau = 0$.

Computer simulations have been run to check (47). Fig. 4 compares theoretical and simulation results with a quaternary alphabet, modulation index $h = 1/2$ and either 1RC or 2RC pulses. The corresponding modified Cramer-Rao bounds

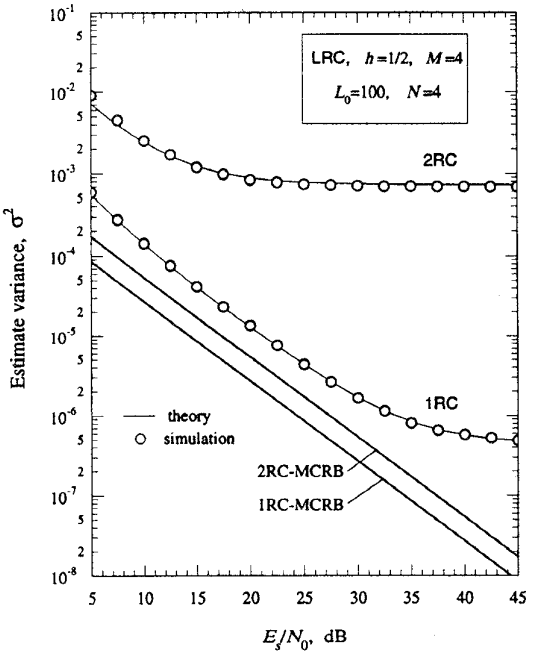


Fig. 4. Timing error variance with quaternary alphabet, $h = 1/2$ and either 1RC or 2RC pulses.

(MCRB) are also shown for reference. The influence of the pulse lenght on the tracking performance is quite apparent. The horizontal floor with $L = 2$ is about three orders of magnitude higher than with $L = 1$. As the situation is even worser with $L \geq 3$, we conclude that the estimator (29) is not suitable with long modulation pulses. In particular, it is not useful with the popular GMSK format which is employed in the GSM digital cellular mobile radio system.

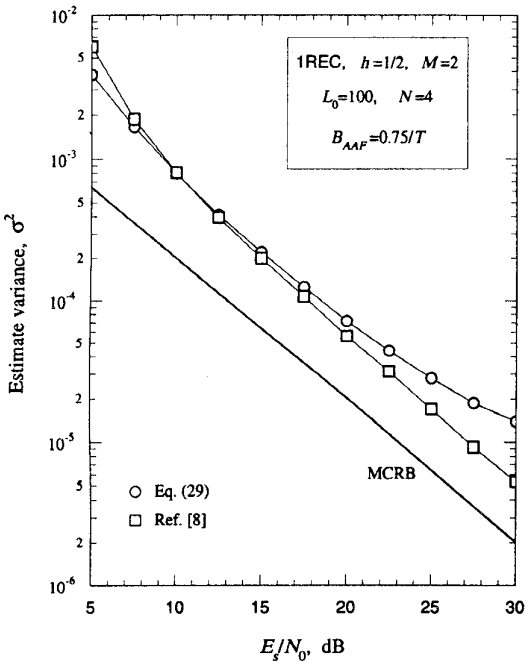


Fig. 5. Comparison between (29) and the estimator in [8].

It is interesting to compare (29) with the timing estimator proposed in [8] for MSK. This estimator is similar to (29) and, in fact, it reads

$$\hat{\tau} = -\frac{T}{2\pi} \arg \left\{ \sum_{n=0}^{N-1} |v(n)| e^{-j2\pi n/N} \right\} \tag{48}$$

with

$$v(n) = \frac{1}{L_0} \sum_{i=0}^{L_0-1} z(iN+n) \qquad n = 0, 1, \cdots N-1 \tag{50}$$

$$z(k) = [x(k)x^*(k-N)]^2. \tag{51}$$

Contrasting (48) with (29) it is seen that the former is simpler to implement. Also, as indicated in Fig. 5, its performance is comparable or slightly better. An obvious question is what happens with modulation indexes *other than* 1/2. Simulations indicate that the performance of [8] degrades rapidly as $h$ departs from 1/2. This is not surprising as [8] has been devised just for MSK. We conclude that, while [8] is particularly suited for $h = 1/2$ and $M = 2$, our algorithm has a more general applicability.

Results pertaining to an octal alphabet and $h = 1/8$ are illustrated in Fig. 6 for 1REC pulses and either coded and uncoded modulation. The solid line is computed from (47) for uncoded data. The coding scheme is based upon a rate-2/3 convolutional encoder over the ring of integers modulo-8, as described in the second line of Table III in [17]. Its gain is 2.13 dB over quaternary CPFSK with $h = 1/4$. It appears that coding has negligible effects on timing recovery. These same conclusions have been arrived at with other codes.

So far we have concentrated on (29). As mentioned earlier, this algorithm is suitable with either a binary alphabet or multilevel alphabets and small modulation indexes. Otherwise, the more complex method (32) must be resorted to. Unfortunately, no analysis is available in the general case and performance has only been assessed by simulation. Figs. 7–8 show variance curves as obtained with (32) for some values of $Q$, the number of terms in the sum (30). Solid lines represent theory only for $Q = 1$. For $Q > 1$ they have been drawn just to ease the reading of the graphs. It is seen that 1RC pulses are much easier to synchronize than 1REC. Also, $Q = 2$ is slightly better than with $Q = 1$ 1RC while it is much better with 1REC. It is worth noting that an observation interval $L_0 = 200$ has been adopted in Fig. 8 to keep $\sigma^2$ small. In general, $L_0$ can be increased even more but, as indicated in remark (7) of previous section, this implies more stringent requirements on symbol and sampling rate stabilities.

## V. Conclusion

Nondata-aided algorithms have been proposed for timing recovery in CPM modulations. They are motivated by maximum likelihood estimation considerations and have a feedforward structure that is suitable for digital implementation. In principle, they can be employed with either binary or multilevel alphabets, with arbitrary modulation indexes and either full or partial response signaling. With short modulator responses their performance is good, sometimes close to the modified Cramer-Rao bound. Limitations arise with smooth pulses, which seem rather hard to deal with. This reminds us of the same trouble encountered in the early studies on synchronization [2].

## Appendix A

In this Appendix, we overview the passages leading to (22)–(23) in the text. As a first step we prove that function

$$F(\Delta t, t) = \prod_{i=-\infty}^{\infty} \frac{1}{M} \frac{\sin[2h\pi M p_{\Delta t}(t-iT)]}{\sin[2h\pi p_{\Delta t}(t-iT)]} \tag{1.I}$$

satisfies the properties

$$F[-\Delta t, t] = F[\Delta t, t + \Delta t], \tag{2.I}$$

$$F[-\Delta t, t] = F[\Delta t, -t]. \tag{3.I}$$

To establish (2.I), start from the definition

$$p_{\Delta t}(t) = q(t) - q(t - \Delta t). \tag{4.I}$$

It is easily seen that $p_{-\Delta t}(t) = -p_{\Delta t}(t + \Delta t)$. Then, substituting into (1.I) yields (2.I). To arrive at (3.I), we write (4.I) in the form

$$p_{-\Delta t}(t) = q(t) - q(t + \Delta t). \tag{5.I}$$

Then, combining with (5) in the text, results in

$$p_{-\Delta t}(t) = -p_{\Delta t}(LT - t) \tag{6.I}$$

from which (3.I) follows, bearing in mind that $F[\Delta t, LT - t] = F[\Delta t, -t]$ since $F[\Delta t, t]$ is periodic with respect to $t$ of period $T$.

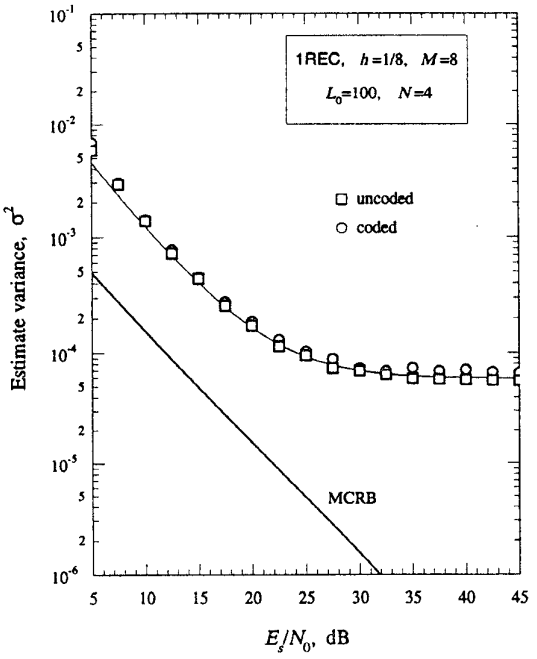


Fig. 6. Timing error variance with octal alphabet, 1REC pulses and $h = 1/8$. The solid line represents analytical results as obtained for uncoded data.

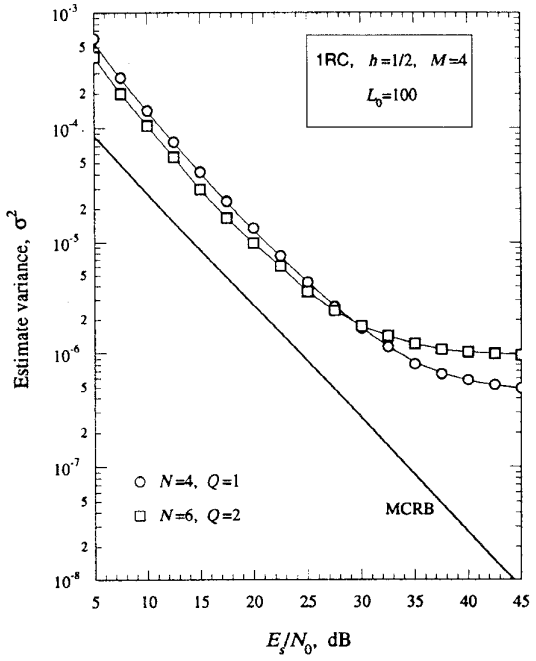


Fig. 7. Timing error variance with quaternary alphabet, 1RC pulses and $h = 1/2$. Marginal improvements are observed in passing from $Q = 1$ to $Q = 2$.

Next, we turn our attention to the coefficients

$$C_m(k_1, k_2) = \frac{1}{T}\int_0^T F[(k_2 - k_1)T_s, k_2T_s - \tilde{\tau}]e^{-j2\pi m\tilde{\tau}/T}\, d\tilde{\tau} \tag{7.I}$$

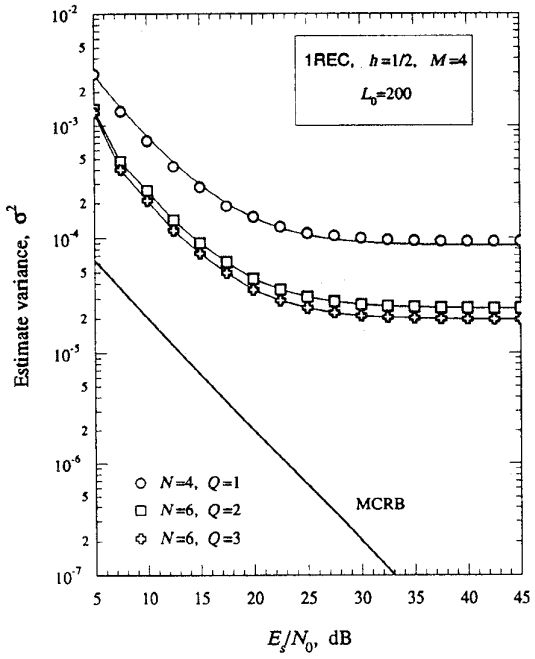


Fig. 8. Timing error variance with quaternary alphabet, 1REC pulses and $h = 1/2$. Significant benefits are gained in passing from $Q = 1$ to $Q = 2$.

in the Fourier series (18). Letting $\tilde{\tau} = k_2T_s - t$ and integrating yields

$$C_m, (k_1, k_2) = c_m(k_2 - k_1)e^{-j2\pi mk_2/N} \tag{8.I}$$

$$c_m(k) = \frac{1}{T}\int_0^T F(kT_s, t)e^{j2\pi mt/T}\, dt. \tag{9.I}$$

As $F[\Delta t, t]$ is real valued, from (9.I) one has

$$c_{-m}(k) = c_m^*(k). \tag{10.I}$$

Also, substituting (2.I)–(3.I) into (9.I) it is found $c_m(-k) = c_m(k)e^{-j2\pi mk/N}$ and $c_m(-k) = c_m^*(k)$. Putting all these facts together it is seen that function

$$h_m(k) = c_m(-k)e^{j\pi mk/N} \tag{11.I}$$

is real valued and satisfies the relationships

$$h_{-m}(k) = h_m(k), \quad h_m(-k) = h_m(k). \tag{12.I}$$

As a third step, combining (8.I) with (11.I) yields

$$C_m(k_1, k_2) = h_m(k_1 - k_2)e^{-j\pi m(k_1+k_2)/N}. \tag{13.I}$$

Then, inserting (13.I) and (18) into (15) results in

$$\Lambda_4(\boldsymbol{x}|\tilde{\tau}) = \sum_{m=-\infty}^{\infty} A(m)e^{j2\pi m\tilde{\tau}/T} \tag{14.I}$$

$$A(m) = \sum_{k_1=0}^{NL_0-1} \sum_{k_2=0}^{NL_0-1} x(k_1) \cdot x^*(k_2) h_m(k_1 - k_2) e^{-j\pi m(k_1+k_2)/N}. \tag{15.I}$$

At this point equation (23) in the text follows by rearranging (15.I). Also, as $h_m(k)$ is real valued, from (12.I) and (15.I) it is seen that $A(-m) = A^*(m)$ and (14.I) becomes

$$\Lambda_4(\boldsymbol{x}|\tilde{\tau}) = A(0) + 2\, Re\left\{ \sum_{m=1}^{\infty} A(m) e^{j2\pi m\tilde{\tau}/T} \right\} \tag{16.I}$$

from which equation (22) is arrived at, dropping $A(0)$ and the factor 2 in front of $\mathrm{Re}\{\cdot\}$.

## Appendix B

This Appendix provides formulas for the coefficients $K_{NN}, K_{SN}$ and $K_{SS}$ in the timing error variance (47). It is assumed that the AAF has a noise bandwidth $B_{\mathrm{AAF}}$ and its transfer function is unity at the origin. The noise correlation coefficient at the output of AAF is denoted $\rho(\xi)$. With a rectangular transfer function, we have $\rho(\xi) = \sin(2\pi B_{\mathrm{AAF}}\xi)/(2\pi B_{\mathrm{AAF}}\xi)$.

All the coefficients have the same structure

$$K_{XY} = \frac{2}{(4\pi N\Gamma)^2} \sum_{k_1=0}^{N-1} \sum_{k_2=0}^{N-1} \sum_{l=-\infty}^{\infty} \sum_{n=-\infty}^{\infty} \sum_{m=-L_0}^{L_0} \cdot \left(1 - \frac{|m|}{L_0}\right) h_1(l) h_1(n) [A_{XY} \cdot \cos(\alpha - \beta) - B_{XY} \cos(\alpha + \beta)] \tag{1.II}$$

where $XY$ stays for either $NN$ or $SN$ or $SS$. Also, $\Gamma$ is a constant given by

$$\Gamma \triangleq \sum_{k=-\infty}^{\infty} |h_1(k)|^2 \tag{2.II}$$

while $\alpha$ and $\beta$ are defined as,

$$\alpha = \frac{\pi}{N}(2k_2 - n) - \frac{2\pi\tau}{T}, \quad \beta = \frac{\pi}{N}(2k_1 - l) - \frac{2\pi\tau}{T}. \tag{3.II}$$

$A_{NN}, A_{SN}, B_{NN}$ and $B_{SN}$ have the expressions

$$A_{NN} = (2B_{\mathrm{AAF}}T)^2 [\rho(k_1 - k_2 - mN)\rho \cdot (k_1 - k_2 - mN + n - l)] \tag{4.II}$$

$$B_{NN} = (2B_{\mathrm{AAF}}T)^2 [\rho(k_1 - k_2 - mN + n)\rho \cdot (k_1 - k_2 - mN - l)] \tag{5.II}$$

$$A_{SN} = 2B_{\mathrm{AAF}}T \{\rho(k_1 - k_2 - mN)F \cdot [(k_2 - k_1 + mN - n + l)T_s, (k_2 - n)T_s - \tau] + \rho(k_1 - k_2 - mN + n - l)F \cdot [(k_2 - k_1 + mN)T_s, k_2T_s - \tau]\} \tag{6.II}$$

$$B_{SN} = 2B_{\mathrm{AAF}}T \{\rho(k_1 - k_2 - mN + n)F \cdot [(k_2 - k_1 + mN + l)T_s, k_2T_s - \tau] + \rho(k_2 - k_1 + mN + n)F \cdot [(k_1 - k_2 - mN + l)T_s, k_1T_s - \tau]\} \tag{7.II}$$

where $F(\Delta t, t)$ is given in (16) in the text. Finally,

$$A_{SS} = \Phi_{l,n}^{-}(k_1T_s - \tau, k_2T_s + mT - \tau) \tag{8.II}$$

$$B_{SS} = \Phi_{l,n}^{+}(k_1T_s - \tau, k_2T_s + mT - \tau) \tag{9.II}$$

with

$$\Phi_{l,n}^{\pm}(t_1, t_2) = \prod_{i=-\infty}^{\infty} \frac{1}{M} \cdot \frac{\sin\{2h\pi M[p_{lT_s}(t_1 - iT) \pm p_{nT_s}(t_2 - iT)]\}}{\sin\{2h\pi[p_{lT_s}(t_1 - iT) \pm p_{nT_s}(t_2 - iT)]\}}. \tag{10.II}$$

## Acknowledgment

The authors would like to thank the anonymous reviewers for their constructive comments which have improved the presentation of the paper.

## References

[1] J. B. Anderson and C.-E. W. Sundberg, "Advances in constant envelope coded modulation," *IEEE Commun. Mag.*, vol. 29, no. 12, pp. 36–45, Dec. 1991.

[2] R. de Buda, "Coherent demodulation of frequency shift keying with low deviation ratio," *IEEE Trans. Commun.*, vol. COM-20, pp. 429–435, June 1972.

[3] S. J. Simmons and P. J. McLane, "Low-complexity carrier tracking decoders for continuous phase modulations," *IEEE Trans. Commun.*, vol. COM-33, pp. 1285–1290, Dec. 1985.

[4] J. M. Liebetreu, "Joint carrier phase estimation and data detection algorithms for multi-h CPM data transmission," *IEEE Trans. Commun.*, vol. COM-34, pp. 873–881, Sept. 1986.

[5] B. A. Mazur and D. P. Taylor, "Demodulation and carrier synchronization of multi-h phase codes," *IEEE Trans. Commun.*, vol. COM-29, pp. 257–266, Mar. 1981.

[6] J. Huber and W. Liu, "Data-aided synchronization of coherent CPM receivers," *IEEE Trans. Commun.*, vol. 40, pp. 178–189, Jan. 1992.

[7] A. N. D'Andrea, U. Mengali, and G. M. Vitetta, "Multiple phase synchronization in continuous phase modulation," in *Digital Signal Processing 3.* New York: Academic, 1993, pp. 188–198.

[8] R. Melhan, Y.-E. Chen, and H. Meyr, "A fully digital feedforward MSK demodulator with joint frequency offset and symbol timing estimation for burst mode mobile radio," *IEEE Trans. Veh. Technol.*, vol. 42, pp. 434–443, Nov. 1993.

[9] A. N. D'Andrea, A. Ginesi, and U. Mengali, "Digital carrier frequency estimation for multilevel CPM signals," in *Proc. ICC'95*, Seattle, WA, June 18–22, 1995.

[10] A. N. D'Andrea, U. Mengali, and R. Reggiannini, "A digital approach to clock recovery in generalized minimum shift keying," *IEEE Trans. Veh. Technol.*, vol. 39, pp. 227–234, Aug. 1990.

[11] U. Lambrette and H. Meyr, "Two timing recovery algorithms for MSK," in *Proc. ICC'94*, New Orleans, LO, May 1994, pp. 918–992.

[12] F. M. Gardner, "Interpolation in digital modems-Part I: fundamentals," *IEEE Trans. Commun.*, vol. 41, pp. 501–507, Mar. 1993.

[13] M. Oerder and H. Meyr, "Digital filter and square timing recovery," *IEEE Trans. Commun.*, vol. 36, pp. 605–611, May 1988.

[14] M. Moeneclaey and G. de Jonghe, "Tracking performance comparison of two ML-oriented carrier-independent NDA symbol synchronizers," *IEEE Trans. Commun.*, vol. 40, pp. 1423–1425, Sept. 1992.

[15] K. Goethals and M. Moeneclaey, "Tracking performance of ML-oriented NDA symbol synchronizers for nonselective fading channels," *IEEE Trans. Commun.*, vol. 43, pp. 1179–1184, Feb./Mar./Apr. 1995.

[16] M. Moeneclaey and I. Bruyland, "The joint carrier and symbol synchronizability of continuous phase modulated waveforms," in *Conf. Rec. ICC'86*, vol. 2, paper 31.5.

[17] R. H.-H. Yang and D. P. Taylor, "Trellis-coded continuous-phase frequency-shift keying with ring convolutional codes," *IEEE Trans. Inform. Theory*, vol. IT-40, pp. 1057–1067, July 1994.

**Aldo N. D'Andrea** (M'82–SM'91) received the Dr.Ing. degree in electronic engineering from the University of Pisa, Italy, in 1977.

From 1977 to 1981, he was a Research Fellow engaged in research on digital phase-locked loops at the Centro Studi per i Metodi e i Dispositivi di Radiotrasmissione of the Consiglio Nazionale delle Ricerche (CNR). Since 1978, he has been involved in the development of the Italian Air Traffic Control Program (ATC). Currently, he is a Full Professor of Communication Systems at the Dipartimento di Ingegneria della Informazione, Università di Pisa. His interests include the design and analysis of digital communication systems, signal processing, and synchronization.

**Umberto Mengali** (M'69–SM'85–F'90) received the Dr.Ing. Degree in electrical engineering from the University of Pisa, in 1961, and the Libera Docenza in Telecommunications from the Italian Education Ministry, in 1971.

Since 1963, he has been with the Department of Information Engineering of the University of Pisa where he is currently a Professor of Telecommunications. His research interests are in digital communication theory, with emphasis on synchronization methods and modulation techniques.

Dr. Mengali is a member of the Communication Theory Committee and a former Editor of the IEEE TRANSACTIONS ON COMMUNICATIONS. He is listed in *American Men and Women in Science*.

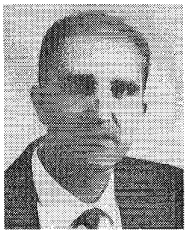

**Michele Morelli** was born in Pisa, Italy, in 1965. He received the Laurea (cum laude) in electronic engineering and the "Premio di Laurea SIP" from the University of Pisa, Italy, in 1991 and 1992, respectively.

Currently, he is involved in the Ph.D. program at the University of Pisa. His interests are in digital communication theory, with emphasis on synchronization algorithms.